Railton, C. J., & Daniel, E. M. (1994). A comparison of the properties of radiating boundary conditions in the FDTD method for finite discretisation and non-planar waves. IEEE Transactions on Antennas and Propagation, 42(2), 276 - 281. 10.1109/8.277225

A Comparison of the Properties of Radiating Boundary Conditions in the FDTD Method for Finite Discretisation and Non-Planar Waves

C. J. Railton and E. M. Daniel

Abstract—**The availability of effective radiating boundary conditions (RBCs) for use with the Finite Difference Time Domain (FDTD) method is essential for the efficient application of the technique to scattering and radiation problems. The majority of published analyses of the behaviour of various RBCs are restricted to the case of plane wave incidence and infinitely fine discretisation, situations which never occur in practice. In this contribution, the behaviour of RBCs in realistic situations is presented and it is shown that the plane wave behaviour is not a good guide as to the behaviour in practical cases. The best RBC for use in general cases is discussed.**

I. INTRODUCTION

The Finite Difference Time Domain (FDTD) method is enjoying a considerable rise in popularity for the analysis of complex geometries such as antennas and scatterers. This is partly due to the increase both in the availability of computer power and the complexity of structures for which analysis is desired. The vast majority of problems to which FDTD is being applied involve open structures which, in turn, require the use of radiating boundary conditions (RBCs) to correctly terminate the computational domain.

Over the last few decades, a number of RBCs have been proposed and several are in common use. The RBCs most often referred to in the literature are those derived by Engquist and Majda [1] with the discretisation given by Mur [2]. These are based on an approximation of the outgoing wave equation by linear expressions using either a Taylor or a Padé approximation. Recently the second order RBC has been extended for application to a non-uniform FDTD grid and to inhomogeneous material. An alternative RBC has been proposed by Higdon [4] and this has recently been applied to the termination of dispersive waveguides [5]. Other RBCs have been proposed by Lindman [6], Reynolds [7] and Liao *et al.* [8] but these appear to be less popular. An alternative approach has been followed by Fang and Mei, [9], [10] who use RBCs to estimate both the E and the H field at a point on the boundary and then combine the results in such a way as to improve the overall accuracy. The technique has been referred to as the Super Absorbing Correction (SAC). Deveze *et. al.* also use a combination of the E and H field estimates in order to reduce the order of the derivatives which neeed to be evaluated. Another technique, used mainly for scattering problems, includes estimating the angle of incidence of the wave by calculation of the Poynting vector [12] and using this information to optimise the RBC parameters.

Although all of these RBCs have been used in conjunction with the FDTD method, little information has been given regarding the relative merits of the different techniques. The information which does exist, eg. [13], [14], [15], is largely restricted to the behaviour of the RBCs with a single incident plane wave although in [14] a line source was also considered. In practice, plane wave incidence is a situation which never occurs. Little guidence exists, therefore, concerning how to choose the best RBC for a particular real problem. In this contribution, the results of a theoretical and numerical investigation into the behaviour and computational efficiency of some existing algorithms are presented, for the more realistic cases of an electric dipole in free space and above a ground plane. In addition the effects of coarse discretisation and non-uniform discretisation on the effectiveness of the different RBCs is investigated.

Manuscript received December 30, 1992; revised August 16, 1993. This work was supported in part by the Science and Engineering Research Council and British Aerospace (Dynamics) Ltd.

The authors are with the Centre for Communications Research, Faculty of Engineering, University of Bristol, Bristol, BS8 1TR, England.

IEEE Log Number 9215648.

II. THEORETICAL BACKGROUND

Of the available second order RBCs which have been described in the literature, the most widely used are those due to Mur [2], Higdon [4] and the super-absorbing RBC eg. [9], [10]. In [16] it is shown that in the limit of infinitesimal discretisation each of these discrete operators is an implementation of (1) or equivalently (2), where the parameters k and v may be freely chosen.

$$\frac{\delta^2 E}{\delta t^2} = v\frac{\delta^2 E}{\delta t \delta x} + kv^2\left(\frac{\delta^2 E}{\delta y^2} + \frac{\delta^2 E}{\delta z^2}\right) \tag{1}$$

$$\frac{\delta^2 E}{\delta t^2} - \frac{v}{1 - v^2k/c^2}\frac{\delta^2 E}{\delta x t} + \frac{v^2 k}{1 - v^2k/c^2}\frac{\delta^2 E}{\delta x^2} = 0 \tag{2}$$

Thus, if the mesh is fine enough, the performance of each of these second order RBCs will be identical. If, however, a realistic value of unit cell size is used, the performance of the RBCs may be significantly different. This was shown to be the case for plane wave incidence in [17]. In order to ascertain the behaviour of the RBCs for non-planar waves, we start from the finite difference description of each. These can be expressed in the form $A(E(r,t), H(r,t)) = 0$ where the functions A are given for Mur's RBC, Higdon's RBC and the super RBC in equations (3)–(5) respectively for the case where the absorbing plane is y–z.

$$\begin{aligned}
&E_z^{n+1}(0,y,z) + E_z^{n-1}(\delta x,y,z)\\
&- C_1\left(E_z^{n+1}(\delta x,y,z) + E_z^{n-1}(0,y,z)\right)\\
&- C_2(E_z^n(0,y,z) + E_z^n(\delta x,y,z))\\
&- C_3(E_z^n(0,y+\delta y,z) - 2E_z^n(0,y,z) + E_z^n(0,y-\delta y,z))\\
&- C_3(E_z^n(\delta x,y+\delta y,z) - 2E_z^n(\delta x,y,z) + E_z^n(\delta x,y-\delta y,z))\\
&- C_4(E_z^n(0,y,z+\delta z) - 2E_z^n(0,y,z) + E_z^n(0,y,z-\delta z))\\
&- C_4(E_z^n(\delta x,y,z+\delta z) - 2E_z^n(\delta x,y,z) + E_z^n(\delta x,y,z-\delta z))
\end{aligned}$$

where

$$C_1 = \frac{v\delta t - \delta x}{v\delta t + \delta x} \quad C_2 = \frac{2\delta x}{v\delta t + \delta x}$$
$$C_3 = \frac{\delta x(v\delta t)^2}{2(\delta y)^2(v\delta t + \delta x)} \quad C_4 = \frac{\delta x(v\delta t)^2}{2(\delta z)^2(v\delta t + \delta x)}$$

$$\begin{aligned}
E^{n+1}(0,y,z) &- 2E^n(\delta x,y,z) + E^{n-1}(2\delta x,y,z)\\
&- (\gamma_1+\gamma_2)(E^n(0,y,z) - E^{n+1}(\delta x,y,z)\\
&- E^{n-1}(\delta x,y,z) + E^n(2\delta x,y,z))\\
&+ \gamma_1\gamma_2(E^{n-1}(0,y,z) - 2E^n(\delta x,y,z)\\
&+ E^{n+1}(2\delta x,y,z))
\end{aligned} \tag{4}$$

where

$$\gamma_1 = \frac{\delta x - v_1\delta t}{\delta x + v_1\delta t} \qquad \gamma_2 = \frac{\delta x - v_2\delta t}{\delta x + v_2\delta t}$$

equivalently

$$\gamma_1 = \frac{\delta x - c\mathrm{Cos}\theta_1 \delta t}{\delta x + c\mathrm{Cos}\theta_1 \delta t} \qquad \gamma_2 = \frac{\delta x - c\mathrm{Cos}\theta_2 \delta t}{\delta x + c\mathrm{Cos}\theta_2 \delta t}$$

The super RBC, which consists of a first order estimate of both the tangential E and H fields together with the basic FDTD algorithm can be expressed as (5).

$$E_z^{n+1}(0,y,z) + (1-k)(E_z^n(\delta x,y,z) + C_1(E_z^{n+1}(\delta x,y,z) - E_z^n(0,y,z)) + kE_z^{2\mathrm{nd}}$$

where

$$E_z^{2\mathrm{nd}} = E_z^n(0,y,z) - \frac{\delta t}{\epsilon} \times \left(\frac{H_x^{n+1/2}(0,y+\delta y/2,z) - H_x^{n+1/2}(0,y-\delta y/2,z)}{\delta y} + \frac{H_{y1} - H_y^{n+1/2}(\delta x/2,y,z)}{\delta x} \right) \tag{5}$$

$$H_{y1} = H_x^{n-1/2}(\delta x/2,y,z) + C_1\left(H_y^{n+1/2}(\delta x/2,y,z) - H_y^{n-1/2}(-\delta x/2,y,z)\right)$$

That the application of the SAC to a first order RBC does none other than yield a second order RBC is demonstrated in [10] although there the effect is described in different terms. The lower curve in Fig. 9 of [10] representing the performance of a first order RBC with SAC is almost identical to the upper curve of Fig. 10 in [10] which represents the performance of a second order RBC without SAC. Similarly the lower curve in Fig. 8 in [10] is almost identical to the upper curve in Fig. 9 in [10], showing that applying the SAC to a perfectly reflecting boundary is an effective, although unorthodox, method of obtaining a first order RBC. It is likely, however that the SAC, if applied to second order Mur or Higdon RBCs, would yield a high order scheme which would be more stable than the Mur or Higdon algorithm of equivalent order.

If a wave of the form $E^i(x,y,z,t)$ is incident on these discretised RBC's then we may define the reflection coefficient by as in (6).

$$R = \frac{A(E^i(x,y,z,t), H^i(x,y,z,t))}{A(E^r(-x,y,z,t), H^r(-x,y,z,t))} \tag{6}$$

where $E^r(-x,y,z,t)$ is the corresponding image wave form (See Fig. 1). This coefficient is a function of the space and time discretisation used in the algorithm as well as the type of RBC used and the spatial distribution of the incident fields close to the boundary plane. For example, for the elementary dipole source, which is used in the tests to be described, the fields are given by (7)(See for example [18]).

$$\begin{Bmatrix} E_x \\ E_y \\ E_z \\ H_x \\ H_y \end{Bmatrix} = \begin{pmatrix} \mathrm{Sin}\theta\mathrm{Cos}\phi & \mathrm{Cos}\theta\mathrm{Cos}\phi & \\ \mathrm{Sin}\theta\mathrm{Sin}\phi & \mathrm{Cos}\theta\mathrm{Sin}\phi & \\ \mathrm{Cos}\theta & -\mathrm{Sin}\theta & \\ & & -\mathrm{Sin}\phi \\ & & \mathrm{Cos}\phi \end{pmatrix} \times \begin{pmatrix} 2Z_0\mathrm{Cos}\theta\left(\frac{1}{r^2} - \frac{j}{r}\right) \\ Z_0\left(\frac{\mathrm{Sin}\theta}{r^2} + \frac{j\beta}{r} - \frac{j}{\beta r^3}\right) \\ \beta\mathrm{Sin}\theta\left(\frac{1}{r} + \frac{j}{r^2}\right) \end{pmatrix} e^{(\pm\beta_x x + \beta_y y + \beta_z z + \beta ct)} \tag{7}$$

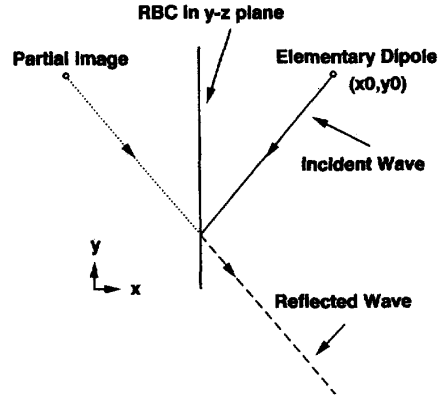

Fig. 1. Geometry for the Theoretical RBC Analysis.

where

$$r = \sqrt{x^2+y^2+z^2}$$

$$\beta_x = \pm\beta\frac{x}{r} \qquad \beta_y = \beta\frac{y}{r} \qquad \beta_z = \beta\frac{z}{r}$$

$$\mathrm{Sin}\theta = \frac{\sqrt{x^2+y^2}}{r} \qquad \mathrm{Cos}\theta = \frac{z}{r}$$

$$\mathrm{Sin}\phi = \frac{y}{\sqrt{x^2+y^2}} \qquad \mathrm{Cos}\phi = \frac{x}{\sqrt{x^2+y^2}}$$

The upper signs correspond to E^i and the lower signs correspond to E^r.

From (7) we can find the values of E^i and E^r at each of the points in space required by (3), (4) or (5), depending on which RBC is under consideration, in order to calculate the values of the function A. The value of R may then be calculated using (6).

III. THEORETICAL ANALYSIS OF RBC BEHAVIOUR

In order to assess the effectiveness of the second order RBCs under practical conditions, tests were carried out for the following cases:

(i) 20 GHz dipole in free space, RBCs placed in the near field at 9 mm.
(ii) 20 GHz dipole in free space, RBCs placed in the far field at 9 cm.
(iii) 20 GHz dipole 3 mm above a ground plane, RBCs placed at 9 mm.

Tests were carried out using the second order RBCs of Mur, Higdon with two different sets of parameters and the SAC. In addition the behaviour of Mur's first order RBC is plotted for comparison. Very fine ($\lambda/200$), fine ($\lambda/20$) and coarse ($\lambda/10$) unit cell sizes were used in order to assess the effect of finite discretisation on the RBC performance. The geometry of the structure under analysis is shown in Fig. 1 and the results of the tests are shown in Figs. 2–6.

From these results we may make the following observations:

(i) For the case where the RBC is placed in the near field of the dipole, there is no significant difference in the performance of the second order algorithms. In particular, the choice of parameters for Higdon's RBC has no effect in this case.
(ii) The behviour of the RBCs when in the far field of the dipole is very similar to that when the incident wave is plane.
(iii) For the case of the dipole above a ground plane and the absorbing plane parallel to the ground plane (Fig. 5), the performance of the RBCs is slightly worse but the difference between the various second order RBCs is still small. Where the absorbing plane is

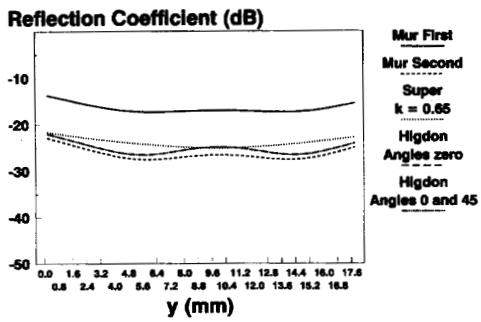

Fig. 2. Theoretical performance of RBCs with single 20 GHz dipole source using uniform /20 grid.

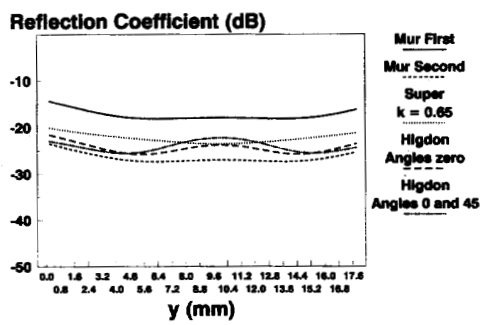

Fig. 3. Theoretical performance of RBCs with single 20 GHz dipole source and uniform /10 grid.

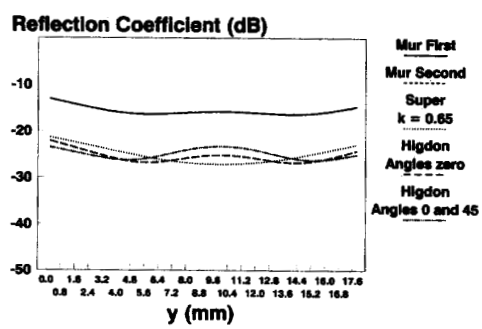

Fig. 4. Theoretical performance of RBCs with single 20 GHz dipole source and uniform /200 grid.

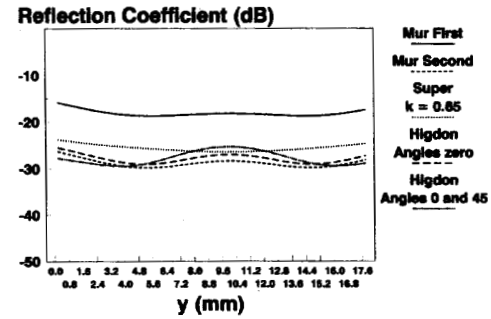

Fig. 5. Theroretical performance of RBCs with a 20 GHz dipole over a ground plane and a uniform /20 grid ($y = 9$ mm).

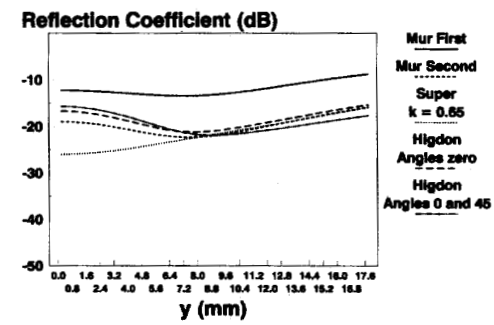

Fig. 6. Theoretical performance of RBCs with a 20 GHz dipole over a ground plane with a uniform /20 grid ($x = 9$ mm).

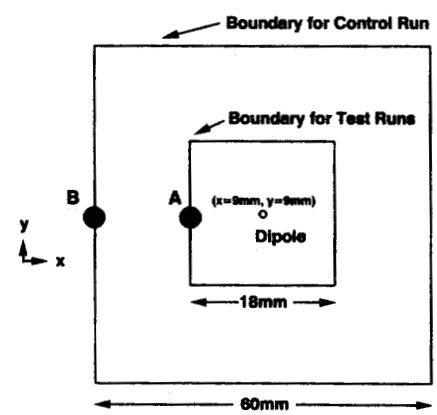

Fig. 7. Geometry for the Numerical RBC Analysis of a single dipole source.

normal to the ground plane (Fig. 6), the SAC performs somewhat better.

(iv) In the far field, the use of a coarser discretisation leads to a deterioration of both Mur's RBC and the SAC. Higdon's RBC is almost unaffected. In the near field coarser discretisation has little effect on any of the RBCs.

IV. NUMERICAL TRIALS OF THE RBCs

In order to see if the foregoing theoretical properties were achieved in an actual FDTD run and to assess the overall performance of the RBCs in a more complex situation, FDTD runs were carried out using the three dimensional geometry whose cross-section is shown in Fig. 7. Unlike the theoretical results presented above, the results from these runs include the effects of multiple reflections from the boundaries and the corners of the computational domain. In addition, the effects of non-uniform gridding and of inhomogenous media can be ascertained.

The first structure used to test the RBCs was that of an infinitesimal dipole surrounded by air and oscillating at 20 GHz which could be compared to the theoretical predictions described in the previous section. This was implemented by exciting the E_z component at the centre of the 18mm cubic mesh with a raised cosine modulated sinusoid. In order to find the level of reflection, a control run, consisting of a much larger (60 mm cube) mesh was used. The

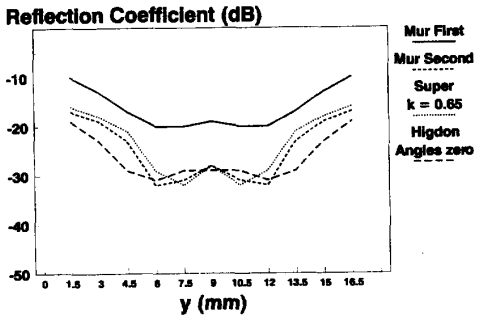

Fig. 8. Numerical performance of RBCs to a single 20 GHz dipole and a uniform /20 grid.

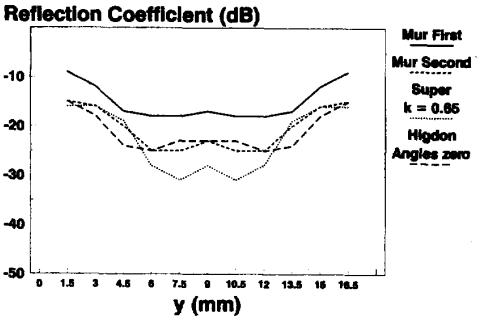

Fig. 9. Numerical performance of RBCs to a single 20 GHz dipole source and a uniform /10 grid.

TABLE I
MESH PARAMETERS FOR THE TEST ON A UNIFORM GRID

	Unit cell size	Number of cells per axis	Width of box (mm)
Control run	0.75	80	60
Test run	0.75	24	18

dimensions of this control run were sufficiently large to ensure that no reflection from the boundaries would enter the test region corresponding to the region for the test runs. The fields in the test region of the control run are, therefore, the true solution to the problem. The fields measured during the test runs are the sum of the true solution and the spurious reflections from the RBCs. Subtracting the test run results for the various RBCs from the control data yields the error. By taking the Fourier Transform of the error and of the control data and dividing one by the other, a value for the reflection coefficient as a function of frequency is obtained. The mesh parameters for both the control and the test runs are given in Table I. These region sizes correspond to a space step of $\lambda/20$ for the source frequency used.

For the control run, the wavefront will hit the centre of each boundary first. The shortest path back to the test region for the reflections is from the points A to B marked in Fig. 7. For the dimensions given in Table I, the path from the source through A to B is 51 mm long. Within the test models the shortest path lengths for multiple reflections between adjacent boundaries are less than 51 mm. Hence the control is large enough that the behaviour of the RBCs including these multiple reflections can be seen.

For the space step used the time step is $dt = 1.37$ pS therefore 124 iterations were needed before the first reflections entered the test region of the control run. Hence, the fields in a plane through the source, in the $x - y$ plane were recorded up to 100 iterations. Five test runs were completed; for Mur's first and second order RBCs, the SAC, with $k = 0.65$ and Higdon's second order RBC, for the angles (0°, 0°) and (10°, 40°).

Fig. 8 shows the reflection coefficients at the boundary nodes along y-z plane. Here it can be seen that the overall behaviour of each of the second order RBCs is similar although the variation along the boundary is slightly different. As before, the choice of θ_1 and θ_2 for Higdon's RBC has virtually no effect on the reflection coefficient.

Comparing Fig. 8 to Fig. 2, we see that although the results are similar, there some differences in detail between the theoretical predictions and the FDTD run. These are due to the fact that in the latter, the reflections from all six RBC planes are observed whereas in Fig. 2, the reflection coefficient, as defined in (6), from a single RBC plane is calculated.

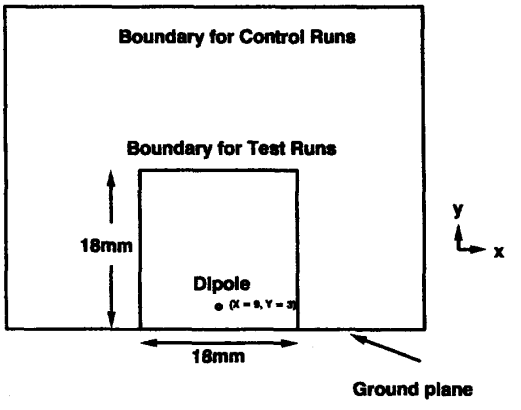

Fig. 10. Geometry for dipole over a ground plane.

In order to assess the effect of using a coarser mesh, similar tests were carried out using a unit cell size of 6 mm, or $\lambda/10$. The results are shown in Fig. 9. Here it can be seen that an overall degredation of approximately 5 dB has occured.

The Effect of using Non-Uniform Grids in Homogeneous Media A second set of tests was performed, only this time the test runs used a graded grid. The test runs used only 1/9 of the nodes used in the fine uniform grid. The non-uniform mesh used for the control and test runs is shown in Table II.

In order to apply Mur's second order RBC to a non-uniform grid, we must use a generalised form of (3). This can be achieved by making use of the discretisation expressed in operator form as (8).

$$D_0^t D_+^x \left(E_{0jk}^n - \frac{1}{2} D_+^t D_-^t (E_{0jk}^n + E_{1jk}^n \right) + \frac{1}{2} (D_+^y D_-^y + D_+^z D_-^z)(E_{0jk}^n + E_{1jk}^n) = 0 \qquad (8)$$

Referring to Fig. 12, it can be shown that the equation relating to E_{z1} is given by (9).

TABLE II
MESH PARAMETERS USED IN THE GRADED GRID TESTS

Region number	Control run region size (mm)	Test run region size (mm)
1	3	6
2	6	3
3	6	3
4	6	6
5	6	
6	3	
7	3	
8	6	
9	6	
10	6	
11	6	
12	3	

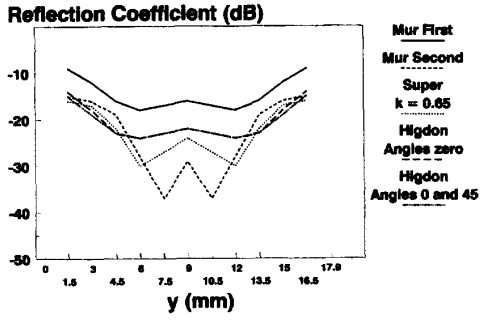

Fig. 11. Numerical performance of RBCs to a uniform 20GHz dipole and a non-uniform grid.

$$
\begin{aligned}
&E_z^{n+1}(0,j,k) + E_z^{n-1}(1,j,k) \\
&\quad + C_1\left(E_z^{n+1}(0,j,k) + E_z^n(0,j,k)\right) \\
&\quad + C_2(E_z^n(0,j,k) + E_z^n(1,j,k)) \\
&\quad + \frac{2C_3}{dy_l + dy_u}(dy_l E_z^n(0,j+1,k) \\
&\quad - (dy_l + dy_u)E_z^n(0,j,k) + dy_u E_z^n(0,j-1,k)) \\
&\quad + \frac{2C_3}{dy_l + dy_u}(dy_l E_z^n(0,j+1,k) \\
&\quad - (dy_l + dy_u)E_z^n(1,j,k) + dy_u E_z^n(1,j-1,k)) \\
&\quad + \frac{2C_4}{dz_l + dz_u}(dz_l E_z^n(0,j+1,k) \\
&\quad - (dz_l + dz_u)E_z^n(0,j,k) + dz_u E_z^n(0,j,k-1)) \\
&\quad + \frac{2C_4}{dz_l + dz_u}(dz_l E_z^n(0,j,k+1) \\
&\quad - (dz_l + dz_u)E_z^n(1,j,k) + dz_u E_z^n(1,j,k-1)) \qquad (9)
\end{aligned}
$$

where

$$C_1 = \frac{v\delta t - \delta x}{v\delta t + \delta x} \quad C_2 = \frac{2\delta x}{v\delta t + \delta x}$$

$$C_3 = \frac{v\delta x(\delta t)^2}{2\delta y_1 \delta y_2 (v\delta t + \delta x)} \quad C_4 = \frac{v\delta x(\delta t)^2}{2\delta z_1 \delta z_2 (v\delta t + \delta x)}$$

The reflection coefficients along the y-z boundary plane are shown in Fig. 11.

It is desirable that an RBC, when used with a graded grid, shall be no worse than when a uniform grid using the graded grid's largest step size is used. The gain in accuracy at the centre of the mesh due to the finer grid may otherwise be negated by the higher levels of boundary reflections. Comparing Fig. 2 and Fig. 3 with Fig. 11 we see that for all RBCs tested, the reflection coefficient for the graded grid is similar to that of the uniform grid. Thus the use of graded grids, at least in this case, presents no problems when used with these RBCs.

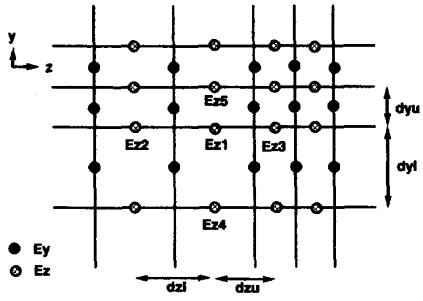

Fig. 12. Non-uniform FDTD mesh.

TABLE III
ARITHMETIC OPERATIONS AND EXTRA MEMORY PER UNIT CELL REQUIRED BY RBC's

RBC	Number of arithmetic operations equivalend additions	Number of reals per field component for history
Mur's First Order	6	2
Mur's Second Order	35	4
Super Absorbing Boundary	29	4
Higdon's Second Order	25	6

V. THE COMPUTATIONAL OVERHEADS INCURRED BY RBCs

To date, comparisons of RBCs have largely concentrated on their reflection coefficients and their stability. Although authors have alluded to the memory and CPU time used, to the authors' knowledge no detailed comparison between the major discrete RBCs has been given. Now that the relative performances of several different RBCs have been compared, it is important to discuss the penalties that each incurs. Although, if a near cubic computational domain is used, the overall effect of computational efficiency of the RBCs is small, for the case where the domain is small in one dimension, such as would be the case for a planar antenna array, the ratio of boundary cells to interior cells is high enough to call for more careful consideration of the overheads involved in the RBCs.

A. The Field History

At each boundary, two tangential field components are estimated. Table III shows how many real numbers are needed to store the history of the field components for the major discrete RBCs under consideration. This is a count per node of the extra memory needed over and above the data already available, and is independent of the grid algorithm used.

A first glance shows that the second order RBCs need at least twice the memory of Mur's first order RBC, which is not unexpected. Immediately, it can be seen that the second order Higdon RBC incurs a 50% greater memory penalty than the other second order RBCs.

B. Number of Operations

Table III shows the number of operations per node per E field component estimated for the same group of discrete RBCs. The coefficients are assumed to have been pre-calculated. For the total

overhead a multiplication or a division has been taken to be equivalent to four additions. Of all the second order operators, the Higdon's RBC is the fastest, that is, less operations are needed. All require more than twice the number of operations as the first order RBC.

VI. Discussion of the Performances of the RBCs

From the analyses and numerical tests presented we may make the following observations:

(i) When used in the near field of a dipole or a pair of dipoles there is little difference in the performance of the second order RBC algorithms. Where differences do exist, they are not predictable *a priori*. In particular, the choice of RBC parameters has negligible effect on performance. This implies that the use of techniques for optimising the parameters of the RBC, such as the calculation of the Poynting vector, [12], is unlikely to be of benefit when carried out in the near field of an antenna or scatterer.

(ii) In the far field of a dipole, the RBCs behave much more like they would with plane wave incidence. For finite discretisation Higdon's RBC is superior to Mur's RBC and the SAC. In this case the choice of parameters does make the expected difference.

(iii) The use of graded grids leads to no deterioration in the performance the RBCs tested.

(iv) The memory requirement for Higdon's RBC is approximately 50% greater than that of the other RBCs tested, the computational load is least for Higdon's RBC and greatest for Mur's RBC, the ratio being 1.4:1.

(v) From the results presented here and in [16], [17] we conclude that where the boundary of the computation domain is in the far field of a radiator or terminates a waveguiding structure that Higdon's RBC gives the best overall efficiency. If the boundary is in the near field of a radiatior than the SAC gives best overall efficiency.

VII. Conclusion

In this contribution we have presented examples of the properties of several well used second order RBCs when used in the near and far fields of a dipole with and without a ground plane. It has been shown that their behaviour is very different to the commonly cited theory for plane wave incidence. In addition a comparison of the required computer resources for the different algorithms has been made. In the case of the boundary being in the near field of a radiator, which occurs often in practice, the RBCs behave similarly and the choice depends only on required computer resources. In this respect, the SAC is superior to Higdon's RBC and Mur's RBC. For waveguide or feedline termination, Higdon's RBC is capable of better performance although it does demand more computer resources than the other RBCs tested.

Acknowledgment

We would like to thank Professor J. P. Mcgeehan of the Centre for Communications Research, University of Bristol for the provision of facilities for this work.

References

[1] B. Engqist and A. Majda, "Absorbing Boundary Conditions for the Numerical Simulation of Waves," *Math. Comp.* vol. 31 pp. 629–651, July 1977.

[2] G. Mur, "Absorbing Boundary conditions for the Finite Difference Approximation of the Time-Domain Electromagnetic-Field Equations," *IEEE Trans EMC-23* pp. 377–382, Nov 1981.

[3] E. M. Daniel and C. J. Railton, "An Improved Second order Radiating Boundary Condition for use with Non-uniform Grids in the Finite Difference Time Domain Method," *proc. 21st EuMC Stuttgart*, pp. 547–552, September 1991.

[4] R. L. Higdon, "Numerical Absorbing Boundary Conditions for the Wave Equation," *Math. Comp.*, vol. 49, pp. 65–91, July 1987.

[5] Z. Bi, K. Wu, C. Wu and J. Litva, "A Dispersive Boundary Conditions for Microstrip Component Analysis using the FDTD Method," *IEEE Trans MTT-40*, April 1992, pp. 774–777.

[6] E. L. Lindman, "Free Space Boundary Conditions for the Time Dependent Wave Equations," *J. Comp. Phys.*, vol. 18, pp. 66–78, 1975.

[7] A. C. Reynolds, "Boundary Conditions for the Numerical Solution of the Wave Propagation Problems," *J. Phys.*, vol. 43, No. 6, pp. 1099,1110, Oct. 1978.

[8] Z. P. Liao, H. L. Wang, B. P. Yang and Y. F. Yuan, "A Transmitting Boundary for Transient Wave Analysis," *Scientia Sinica (Series A)*, vol. 27, pp. 1063–1076, October 1984.

[9] J. Fang and K. K Mei, "A Super-Absorbing Boundary Algorithm for Solving Electromagnetic Problems by the Time Domain Finite Difference Method," *Dig. IEEE AP-S Symposium 1988*, pp. 472–475.

[10] K. K. Mei and J. Fang, "Superabsorbtion—A method to improve Absorbing Boundary Conditions," *IEEE Trans AP-40*, September, 1992, pp. 1001–1010.

[11] T. Deveze, F. Clerc and W. Tabbara, "Second Order Pseudo-Transperent Boundary Equations for the FDTD method," *IEEE AP-S Symposium* 1990, pp. 1624, 1627.

[12] C. L. Britt, "Solution of Electromagnetic Scattering Problems using Time Domain Techniques," *IEEE Trans MTT-37*, pp. 1181–1192, Sept. 1989.

[13] F. X. Canning, "On the Application of some Radiation Boundary Conditions," *IEEE Trans AP-38*, pp. 740–745, May 1990.

[14] T. G. Moore, J. G. Blaschlak, A. Taflove and G. A. Kriegsmann, "Theory and Application of Radiation Boundary Operators," *IEEE Trans AP-36*, December 1988, pp. 1797–1812.

[15] J. G. Blaschak and G. A. Kriegsmann, "A Comparative Study of Absorbing Boundary Conditions," *J. Comput. Physics*, vol. 77, pp. 109–139, July 1988.

[16] C. J. Railton, E. M. Denial, D. L. Paul and J. P. McGeehan, "Optimised Absorbing Boundary Conditions for the Analysis of Planar Circuits using the Finite Difference Time Domain Method," To be published *IEEE Trans MTT-41*, pp. 290–297, Feb. 1993.

[17] C. J. Railton and E. M. Daniel, "Comparison of the Effect of Discretisation on Absorbing Boundary Algorithms in the Finite Difference Time Domain Method," *Electronics Letters*, vol. 28, No. 20, 24th September 1992, pp. 1891–1893.

[18] S. E. Schwarz, "Electromagnetics for Engineers," Saunders College Publishing, 1990, pp. 348–349.